HHS Public Access

Author manuscript

Biotechnol Bioeng. Author manuscript; available in PMC 2015 June 22.

Published in final edited form as:

Biotechnol Bioeng. 2014 April ; 111(4): 829–841. doi:10.1002/bit.25145.

The Potential of Encapsulating "Raw Materials" in 3D Osteochondral Gradient Scaffolds

Neethu Mohan[1], **Vineet Gupta**[2], **BanuPriya Sridharan**[2], **Amanda Sutherland**[2], and **Michael S. Detamore**[2,3]

[1]Division of Tissue Engineering and Regeneration Technologies, Biomedical Technology Wing, Sree Chitra Tirunal Institute for Medical Sciences and Technology, Trivandrum, Kerala, India

[2]Bioengineering Graduate Program, University of Kansas, Lawrence, Kansas

[3]Department of Chemical and Petroleum Engineering, University of Kansas, Lawrence, Kansas

Abstract

Scaffolds with continuous gradients in material composition and bioactive signals enable a smooth transition of properties at the interface. Components like chondroitin sulfate (CS) and bioactive glass (BG) in 3D scaffolds may serve as "raw materials" for synthesis of new extracellular matrix (ECM), and may have the potential to completely or partially replace expensive growth factors. We hypothesized that scaffolds with gradients of ECM components would enable superior performance of engineered constructs. Raw material encapsulation altered the appearance, structure, porosity, and degradation of the scaffolds. They allowed the scaffolds to better retain their 3D structure during culture and provided a buffering effect to the cells in culture. Following seeding of rat mesenchymal stem cells, there were several instances where glycosaminoglycan (GAG), collagen, or calcium contents were higher with the scaffolds containing raw materials (CS or BG) than with those containing transforming growth factor (TGF)-β3 or bone morphogenetic protein (BMP)-2. It was also noteworthy that a combination of both CS and TGF-β3 increased the secretion of collagen type II. Moreover, cells seeded in scaffolds containing opposing gradients of CS/TGF-β3 and BG/BMP-2 produced clear regional variations in the secretion of tissue-specific ECM. The study demonstrated raw materials have the potential to create a favorable microenvironment for cells; they can significantly enhance the synthesis of certain extracellular matrix (ECM) components when compared to expensive growth factors; either alone or in combination with growth factors they can enhance the secretion of tissue specific matrix proteins. Raw materials are promising candidates that can be used to either replace or be used in combination with growth factors. Success with raw materials in lieu of growth factors could have profound implications in terms of lower cost and faster regulatory approval for more rapid translation of regenerative medicine products to the clinic.

Correspondence to: M.S. Detamore, telephone: 785-864-4943; fax: 785-864-4967; detamore@ku.edu.

Conflicts of interest: none.

Supporting Information

Additional supporting information may be found in the online version of this article at the publisher's web-site.

Keywords

gradients in signals; raw materials; chondroitin sulfate; osteochondral tissue engineering; microsphere-based scaffold

Introduction

A continuously graded osteochondral construct that simultaneously regenerates both cartilage and bone in addition to promoting proper integration at the interface is a promising approach to firmly anchor a cartilage substitute to surrounding tissues. Three-dimensional (3D) microsphere-based scaffolds with gradients of signals that can guide the chondrogenic and osteogenic differentiation of cells in different regions of the same matrix have been found to be a suitable candidate for osteochondral regeneration (Dormer et al., 2010, 2012). Our previous studies have indicated that 3D microsphere-based scaffolds with gradients in signals have the ability to control patterning of cell phenotype and secrete tissue-specific ECM components to promote osteochondral regeneration (Dormer et al., 2010, 2011, 2012; Mohan et al., 2011).

It has been reported that chondroitin sulfate (CS), a major component of cartilage tissue, when included in a 3D scaffold, generated a favorable microenvironment for chondrocytes and enhanced glycosaminoglycan (GAG) and collagen production in vitro and promoted faster regeneration in vivo (Chen et al., 2007; Fan et al., 2006). Similarly, bioactive glasses (BG) are widely known for their ability to bond directly to bone (Hench and Thompson, 2010), and their ionic dissolution products (e.g., Si, Ca, P) are found to stimulate the expression of several genes of osteoblasts (Fu et al., 2010; Hoppe et al., 2011; Rahaman et al., 2011; Will et al., 2012; Xynos et al., 2001). Qiu et al. (2000) reported that the surface of the BG encapsulated in poly lactic acid microsphere was fully transformed into carbonated calcium hydroxyapatite after 3 weeks of immersion in simulated physiological fluid. Our interests were on evaluating the cell response in scaffolds made from sintered microspheres, encapsulated with growth factors, raw materials, their combinations, and with gradients in these signals. Encapsulation of simple raw materials within the microspheres is a promising approach to generate scaffolds, with inherent niches that favor faster synthesis of tissue specific proteins. They can be used to recreate biomimetic environment in 3D scaffolds and may serve as an alternative to expensive growth factors to accelerate the tissue regeneration. Success with raw materials in lieu of growth factors could have profound implications in terms of lower cost and faster regulatory approval for more rapid translation of regenerative medicine products to the clinic.

In this study, we investigated whether the encapsulation of the ECM component CS and an osteoinductive signal, BG, in 3D microsphere-based scaffolds can act as a supply of “raw materials” (Renth and Detamore, 2012) and simultaneously provide building blocks to regenerating tissue and favor faster matrix synthesis and mineralization of an osteochondral scaffold. Three-dimensional scaffolds were fabricated using biodegradable poly($_{D,L}$-lactic-co-glycolic acid) (PLGA) microspheres that encapsulated chondrogenic and osteogenic growth factors, raw materials, and their combinations. Osteochondral scaffolds with gradient

signals and raw materials were also fabricated using a gradient technology we first reported in Singh et al. (2008). The response of mesenchymal stem cells to growth factors, raw materials, and their combinations, as well as the response to gradient signals for osteochondral regeneration, was investigated in this study. Cell response to chondrogenic and osteogenic growth factors; transforming growth factor (TGF)-β3 or bone morphogenetic protein (BMP)-2, encapsulated in microspheres have been studied in detail in our earlier work (Dormer et al., 2010; Mohan et al., 2011). These groups with the bioactive signals have been included in the present study and compared to the raw material encapsulated groups.

Materials and Methods

Materials

Poly(D,L-lactic-co-glycolic acid) (PLGA) (50:50 lactic acid: glycolic acid, acid end group, MW *42,000–44,000 Da) of intrinsic viscosity (i.v.) 0.35 dL/g was obtained from Lakeshore Biomaterials (Birmingham, AL). TGF-β3 and BMP-2 were obtained from Peprotech, Inc. (Rocky Hill, NJ), chondroitin 4 sulfate (lyophilized powder of CS A sodium salt from bovine trachea) was obtained from Sigma (St. Louis, MO), and BG powder 45S5 (10 micron size powder) was obtained from MO-SCI Healthcare (Rolla, MO). All other reagents and organic solvents utilized were of cell culture or ACS grade.

Fabrication of Microspheres

Seven different sets of microspheres were fabricated for the whole study: (1) PLGA microspheres; chondrogenic microspheres were either (2) TGF-β3 encapsulated microspheres (PLGA-TGF), (3) CS-encapsulated microspheres (PLGA-CS), or (4) microspheres with a combination of TGF-β3 & CS encapsulated (PLGA-TGF-CS); and osteogenic microspheres were either (5) BMP-2 encapsulated microspheres (PLGA-BMP), (6) bioactive glass encapsulated microspheres (PLGA-BG) or (7) a combination of BMP-2 and BG encapsulated (PLGA-BMP-BG) microspheres. For preparation of the growth factor-loaded microspheres, TGF-β3 was reconstituted in a buffer of 10 mM citric acid diluted in 0.1% bovine serum albumin (BSA), and BMP-2 was reconstituted in 0.1% BSA. The reconstituted protein solutions were individually mixed with PLGA dissolved in dichloromethane (DCM) (20% w/v) at a loading ratio of 30 ng TGF-β3 or 60 ng BMP-2 per 1.0 mg of PLGA (Mohan et al., 2011). The final mixture was then sonicated over ice (50% amplitude, 20 s). The PLGA-CS microspheres were fabricated by adding 4% (w/v) CS to 16% (w/v) PLGA in DCM, and PLGA-TGF-CS had 30 ng of TGF-β3/mg PLGA in addition to CS. The osteogenic microspheres contained 2% (w/v) BG, 18% (w/v) PLGA, and PLGA-BMP-BG had BMP-2 at a concentration of 60 ng/mg PLGA. Using PLGA-growth factors/CS/BG emulsions, microspheres were prepared following technology that we previously reported (Dormer et al., 2012; Mohan et al., 2011; Singh et al., 2008). Using acoustic excitation produced by an ultrasonic transducer, regular jet instabilities were created in the polymer stream that produced uniform polymer droplets (Berkland et al., 2001; Singh et al., 2008). The particles were collected, washed, and further lyophilized for 48 h.

Fabrication of Gradient and Homogeneous Scaffolds

Gradient scaffolds ("GRADIENT" group) were prepared using our previously reported technology (Dormer et al., 2012; Mohan et al., 2011; Singh et al., 2008). Briefly, lyophilized microspheres (50–100 mg) of two different types; PLGA-TGF-CS and PLGA-BMP-BG were dispersed in distilled water and separately loaded into two syringes. The suspensions were pumped at opposing flow rates into a cylindrical glass mold (diameter = 3.8 mm) in a controlled manner using programmable syringe pumps (PHD 22/2000; Harvard Apparatus, Inc., Holliston, MA). Using a filter at the bottom of the mold, distilled water was filtered, where the microparticles stacked in the mold until a height of 3–4mm was reached. The scaffolds were 3.2–3.5mm in diameter and 3–4mm in height. The profile for gradient constructs was linear, where the top one-fourth of the total height was comprised of chondrogenic microspheres (PLGA-TGF-CS) only (0.75 mm), then the next one-fourth (0.75 mm) was a linear transition from chondrogenic (PLGA-TGF-CS) to osteogenic (PLGA-BMP-BG) microspheres, and the bottom half (1.5 mm) contained only osteogenic microspheres (PLGA-BMP-BG). The stacked microspheres were then sintered using ethanol-acetone (95:5 v/v) for 45 min. The scaffolds were further lyophilized for 48 h and were sterilized with ethylene oxide for 12 h. The control PLGA and other homogenous scaffolds, abbreviated as TGF, CS, TGF-CS, BMP, BG, and BMP-BG, were fabricated by packing them into molds of desired size, followed by sintering. The homogeneous scaffolds used for cell seeding had uniform dimension 3.2–3.5 mm in diameter and 3.5 mm in height. The microspheres used for the fabrication of different types of scaffolds and their compositions are represented in Table I. Eight different groups were used for the study: PLGA, TGF, CS, TGF-CS, BMP, BG, BMP-BG, and GRADIENT. The scaffolds used for each analysis are represented in Table II.

Scanning Electron Microscopy with Energy Dispersion Spectroscopy

The surface morphology of PLGA, PLGA-CS, and PLGA-BG microspheres were analyzed using LEO 1550 field emission scanning electron microscopy (SEM). The microspheres were cryofractured using a sharp blade to image the morphology of the cross section. The dispersion of CS and BG on the surface or within the microspheres was further analyzed using LEO 1550 field emission SEM with an energy dispersive spectroscopy (EDS) using a SiLi detector at a 20 kV accelerating voltage. Pixel maps were generated using an EDS genesis software package, (EDAX, Inc., Mahwah, NJ). The PLGA microspheres were also imaged as a control to confirm the absence of Si as a contaminant in the EDS map.

MicroCT

The 3D structures of PLGA, CS, and BG scaffolds were imaged using a high-resolution microcomputed tomography (MicroXCT-400, Xradia, Inc., Concord, CA). The transmission X-ray imaging of the samples was performed using an X-ray tube with a tungsten anode setting of 50–60 kV at 8 W with an optical magnification of × 10. The 3D images were reconstructed with the help of "XM Reconstructor 8.0" software (Xradia, Inc.) using images taken at an exposure time of 5 s per image. Video files were generated from the reconstructed images obtained from the microCT data using "XM 3D viewer" software (Xradia, Inc.).

Release of Chondroitin Sulfate from CS Scaffolds

The release of chondroitin sulfate from the CS scaffolds was studied by incubating the unseeded scaffolds in 500–1000 μL of PBS at 37°C. The different end points were week 0 (24 h), week 2, week 4, and week 6. At the respective time points the PBS was aspirated and used to estimate the total amount of CS released. The amount of CS retained within the scaffolds was determined by solubilizing the polymer in 200 μL of methylene chloride. To this DI water was further added to extract the CS to the aqueous phase. The amount of CS present in the aqueous phase and that retained within the hydrophobic phase was estimated using dimethyl methylene blue (DMMB) assay kit (Biocolor, Newtownabbey, Northern Ireland) according to the manufacturer's instructions. The study was performed with a sample size of $n = 3–4$.

Cell Seeding of Scaffolds

Rat bone marrow stem cells (rBMSCs) were obtained from the femurs of 15 young male Sprague–Dawley rats (176–200 g, SASCO) following a University of Kansas approved IACUC protocol (175–08). The cells at passage 4 were resuspended in culture medium at a concentration of 30×10^6 cells/mL. Forty microliter of cell suspension (~1.2×10^6 cells) was added to each scaffold and cells were allowed to attach for 1 h. Two milliliter of culture medium (αMEM supplemented with 10% FBS (Certified, cat #16000–036), 1% antibiotic, 15 mM HEPES buffer (Invitrogen Life Technologies, Carlsbad, CA)) was added after 1 h. The medium was replaced for all constructs every 48 h. The constructs were withdrawn from culture and used for the analyses as represented in Table II. The "week 0" time point indicated constructs 24 h after seeding. At week 0, only three scaffold types: PLGA, CS, and BG scaffolds that do not contain growth factors were used for the analyses. At week 0, week 3, and week 6, constructs were evaluated for biochemical content and mechanical integrity. Week 6 samples were also evaluated with histology.

Biochemical Analyses

At weeks 0, 3 and 6; cell-seeded constructs were crushed, homogenized and digested using papain. The total GAG content was estimated using a dimethylmethylene blue (DMMB) assay kit according to the manufacturer's instructions (Biocolor). Total hydroxyproline (HYP) was estimated using a modified hydroxyproline assay (Edwards and O'Brien, 1980), and the calcium content was estimated in samples homogenized and incubated in 0.05% triton X 100 using a QuantiChrom™ Calcium Assay Kit (DICA-500; QuantiChrom, Hayward, CA). Biochemical analyses were performed with a sample size of $n = 3–5$.

Histological and Immunohistochemical Staining

For histology, the week 6 constructs were embedded in optimal cutting temperature (OCT, Tissue-Tek, Torrance, CA) embedding medium; 12 μm thick sections were cut using a cryostat (Micron Hm-550 OMP, Vista, CA) and stained using Safranin O for GAGs and Alizarin red for bone mineralization. The sections were also stained for the presence of collagen types I and II using immunohistochemistry. Mouse monoclonal anti-collagen type I (1:1,500 dilution; Accurate Chemical and Scientific, Westbury, NY) and mouse monoclonal anti-collagen type II (1:1,000 dilution; Chondrex, Redmond, WA) primary antibodies were

used for the immunostaining. The primary antibodies were followed by a secondary antibody, and the VectorABC complex, and visualized with the DAB substrate (Vector Laboratories, Burlingame, CA) as per the manufacturer's protocol. Negative controls were run with the primary antibody omitted.

Mechanical Testing

Mechanical characterization of the constructs was carried out using a uniaxial testing apparatus (Instron Model 5848, Canton, MA, 50 N load cell) under unconfined compression using a custom-built bath-platen apparatus (Singh and Detamore, 2009). The dimensions of the constructs used for mechanical testing are indicated in Table III. The constructs were tested under hydrated conditions, in phosphate buffered saline (PBS) at 37°C. A tare load 0.01 N and a continuous deformation rate of 1 mm/min was used during the compression testing. Compressive moduli of elasticity were calculated from the linear regions of the stress-strain curves. Mechanical testing was performed with a sample size of $n = 3$.

Statistical Analysis

Statistical analyses were performed using a single factor analysis of variance (ANOVA) with a Tukey's post-hoc test using GraphPad Prism version 5.02 for Windows, (GraphPad software, La Jolla, CA). All quantitative results were expressed as the average ± standard deviation. Values of $P < 0.05$ were considered significant.

Results

Characterization of 3D Scaffolds

Figure 1 represents the scanning electron micrographs of PLGA, PLGA-CS, and PLGA-BG microspheres. The PLGA microspheres were smooth on the surface while the CS and BG encapsulated microspheres had minute micron size pores on the surface and inside. The PLGA and PLGA-CS microspheres retained their spherical shapes, while the PLGA-BG microspheres had the shape of a deflated soccer ball. The high-magnification SEM images and the EDS mapping data for the sulfur (S) on the cross section of PLGA-CS microspheres indicated virtually uniform dispersion of CS within the microspheres (Fig. 1). Bioactive glass particles were observed both on the surface and on the broken pieces of the deflated PLGA-BG microspheres. The EDS mapping data for silicon (Si) also indicated the presence of BG on the surface of PLGA-BG microspheres (Fig. 2). The absence of peak for Si on the EDX spectrum and the negligible values for elemental composition confirmed the absence of Si on the control PLGA microspheres (Supplementary Fig. 1). The 3D reconstructed microCT images (Fig. 3) and the video generated from the microCT data (supplementary video files S1, S2, and S3) indicated that the void spaces between the spheres acted as pores, and the pores were open and interconnected. The microCT images also confirmed that the PLGA-CS and PLGA-BG microspheres were porous as indicated by the SEM data.

Release of Chondroitin Sulfate from the CS Scaffolds

Figure 4 represented the release profile of CS and the amount retained within the CS scaffolds. An initial release of 6% was observed at week 0 and the cumulative percentage released was 15% by week 2. Further at week 4, the percentage cumulative release was 16%

and at week 6 there was a total of 24% release from the scaffolds. At week 0, most of the CS (79%) was present in the polymer phase and very less amount (15%) of the CS was extracted into the aqueous phase. At week 2 and week 4 the amount of CS in the polymer phase showed a decrease though there was no significant change. At week 6 there was an increase in the CS content in the aqueous extract.

Biochemical Analysis of the 3D Constructs

The total GAG, HYP, and calcium contents of constructs at week 0, week 3, and week 6 are represented in Figure 5. The GAG contents at week 0 (values 24 h after cell seeding) were measured only for the three types of scaffold that did not contain a growth factor: PLGA, CS, and BG. The GAG contents of both the CS and TGF-CS groups at week 3 were three times higher than those of the CS group at week 0 ($P < 0.0001$) and all other groups at week 3 ($P < 0.0001$). There was no significant difference in GAG content between CS and TGF-CS at week 3. It must be emphasized that the values of CS and TGF-CS obtained from the biochemical analysis represented the GAGs present in the ECM secreted by the cells, as well as the encapsulated chondroitin released and entrapped within the ECM at each time point. The GRADIENT constructs showed higher values when compared to control PLGA, growth factor loaded, and BG encapsulated groups. On comparing the week 3 and week 6 values, the total GAG contents of the CS, TGF-CS, and GRADIENT groups were 6.7 ($P < 0.0001$), 6.9 ($P < 0.0001$), and 5.7 ($P < 0.0001$) times larger at 3 weeks than at 6 weeks, respectively. However, there were no significant changes from 3 to 6 weeks in the total GAG contents in other groups.

At the week 6-time point, all of the encapsulated raw material and the GRADIENT scaffolds had significantly higher values when compared to the PLGA, TGF, and BMP groups. At week 6, the CS and TGF-CS groups had three times the GAG content, and the BG, BMP-BG and GRADIENT groups had two times the GAG content of the PLGA group ($P < 0.0001$). Similarly, the GAG contents of the BG, BMP-BG, and GRADIENT groups were three times higher than that of the TGF group ($P < 0.0001$), while the CS and TGF-CS groups had five times higher GAG contents than the TGF group ($P < 0.0001$) at week 6. Furthermore, the CS and TGF-CS groups had GAG contents 7 and 7.7 times higher, and the BG, BMP-BG, and GRADIENT groups had GAG contents 5 times higher than the BMP group ($P < 0.0001$). The CS had 1.3 times more GAGs than the BG and the GRADIENT groups ($P < 0.0001$) and 1.5 times more GAGs than the BMP-BG group ($P < 0.0001$); while the TGF-CS group had 1.5 times higher values than the BG and the GRADIENT groups ($P < 0.0001$), and 1.6 times higher values than the BMP-BG ($P < 0.0001$).

At week 3, the HYP content of the BMP-BG group was 21, 19, 11, 58, 31, and 16 times higher than those of the groups PLGA, CS, TGF, TGF-CS, BMP, and BG ($P < 0.0001$), respectively. The HYP content of the GRADIENT group was 10, 9, 5, 27, 14, 7 times higher than those of the PLGA, CS, TGF, TGF-CS, BMP, and BG groups ($P < 0.0001$), respectively. When compared to the control week 0 constructs, the HYP content of the BMP-BG group was 21, 11, 13 times higher than those of the PLGA, CS, and BG groups ($P < 0.0001$), respectively. The HYP content of the GRADIENT group at week 3 had 6 times higher than at week 0 ($P < 0.0001$). At week 6, the HYP contents of the CS, TGF-CS, BMP,

and BG groups were 6 ($P < 0.0001$), 28 ($P < 0.0001$), 19 ($P < 0.0001$) and 6 ($P < 0.0001$) times greater than they were at 3 weeks, respectively. However, the HYP content of the BMP-BG group was 23 times larger at week 3 than at week 6 ($P < 0.0001$).

The total calcium content of the BG group was 1.9 times higher at week 3 than at week 0 ($P < 0.0001$. This 3-week calcium content in the BG group was 3.7, 2, 2.5, 2.1, 1.6, 1.5 times higher than in the PLGA, TGF, BMP, TGF-CS, BMP-BG, and GRADIENT groups, respectively ($P < 0.0001$). The calcium contents of the TGF, BMP-BG, and GRADIENT groups were 1.5, 2, and 2.5 times higher than that of the control PLGA group at week 3 ($P < 0.0001$). At week 6, all of the groups showed a decrease in the total calcium content when compared to the week 3 constructs; however, the difference was not significant except in the BG group, where the week 3 value was 4.3 times higher ($P < 0.0001$). At week 6, the BG group had two times more calcium than most of the other groups.

Dimensions and Mechanical Testing of the 3D Constructs

Table III represents the dimensions of constructs used for mechanical testing. There was a massive increase in the scaffold dimensions from week 0 to week 3 due to excessive swelling. This was followed by a decrease in the dimensions in next 3 weeks. In case of PLGA, the excessive swelling and massive degradation resulted in total distortion of the scaffold structure at week 3 and these constructs appeared as a thin 2D film by the end of week 6; and modulus could not be measured. The total volume of TGF increased five times from week 0 to week 3 and further decreased five times from week 3 to week 6. Similarly, the volume of BMP increased 3.5 from week 0 to week 3 and showed a same decrease in volume from week 3 to week 6. The difference in swelling and the rates of degradation created variations in the dimensions of the constructs at different end points and a specific aspect ratio could not be maintained for the mechanical testing. The differences in aspect ratios may have contributed to differences in moduli.

The compressive moduli of PLGA, CS, and BG scaffolds were measured in hydrated conditions at 37°C. The results are represented graphically in Figure 6. There were no significant differences among the groups at both week 3 and week 6. The compressive modulus decreased at week 3 followed by an increase in all the constructs at week 6; except for CS and BG. However these differences were not significant. The increase in BMP-BG from week 0 to week 6 was significant.

Histology and Immunostaining of the Constructs

The Saf-O staining and immunostaining for collagen type II for all groups at week 6 are represented in Figure 7, and the Alizarin red staining and immunostaining for collagen type I are represented in Figure 8. PLGA constructs showed very weak staining with Saf-O, while the exclusively growth factor encapsulated groups, TGF and BMP, showed an uneven Saf-O staining. The CS-encapsulated constructs, CS and TGF-CS, showed more uniform and deeper Saf-O staining relative to all other groups. The BMP-BG constructs showed mild Saf-O staining, while the BG constructs showed Saf-O staining only along the periphery of the sections. The GRADIENT groups showed deeper Saf-O staining at the chondrogenic region of the constructs followed by a gradual decrease in the intensity at the interface and

almost negligible GAG towards the osteogenic region. Alizarin red staining for calcium was observed in almost all of the constructs, but the staining intensity varied among the constructs. The BG and BMP-BG constructs showed the deepest Alizarin red staining, moreso than even the BMP group. The GRADIENT constructs also showed deep Alizarin red staining, which was deeper in the osteogenic region than in the chondrogenic region, although calcium deposition was observed at a few sites in the chondrogenic region of the GRADIENT constructs. The immunostaining data indicated secretion of collagen type II in the TGF and TGF-CS constructs; however, the CS constructs had very low and non-uniform staining. TGF-CS constructs showed deeper collagen type II staining than all of the other constructs. Both the BMP and BG constructs showed positive staining for collagen type II, but the staining pattern was non-uniform and was confined to the edges of the sections. The BMP-BG constructs showed negligible collagen type II staining, while the GRADIENT groups had a higher staining intensity for collagen type II at the chondrogenic region of the constructs. At week 6, the PLGA constructs showed positive staining for both the collagen types. The TGF, BMP, and BG constructs showed positive immunostaining of collagen type I, while the CS and BMP-BG groups showed negligible collagen type I staining. The GRADIENT constructs showed mild staining for collagen type I in both the chondrogenic and osteogenic regions.

Discussion

Raw material encapsulation altered the appearance, structure, porosity, and degradation of the scaffolds. PLGA microspheres had a smooth surface, while both the CS and BG encapsulated microspheres had sub micron pores on the surface and inside. The pores in these microspheres might have been formed due to the solvent removal process during the fabrication step. The CS and the BG particles were distributed nearly homogeneously on the microspheres. The PLGA and PLGA-CS microspheres had spherical shapes, while the PLGA-BG microparticles had the shape of a deflated soccer ball. PLGA-BG microspheres remained stable during the initial fabrication step and deflation of the microspheres were observed after the hardening or lyophilization process; probably due to removal of solvent at different rates from the core and the periphery. During this process there might have been slight phase separation leading to a polymer-bioactive glass lean phase at the core and the polymer-BG rich phase wards the periphery. This might have generated a structural instability leading to a weak core that resulted in a deflated soccer ball like structure of the microsphere. Qiu et al. (2000) have reported the fabrication of stable PLA-modified BG microspheres by solid-in-oil-in-water emulsion and solvent removal method. They used a polymer-composite mixture containing equal quantity of PLA and the modified BG mixture, for the fabrication. Micron-size pores were observed on the microsphere surface and on the cross section due to solvent removal process and were similar to our observations. The bio-glass powders were distributed throughout the porous polymer matrix. Lu et al. (2003) also fabricated PLGA-BG microspheres with higher BG content than the amount used in our study. The higher concentration of BG used in these studies might have contributed to a uniform packing density of polymer-composite from the core to the periphery of the microspheres resulting in a stable structure of the microsphere.

Our Micro CT data indicated that the microspheres were sintered at the points of contact to form a 3D connected matrix. The solvent sintering was standardized to allow plasticization of PLGA at these points of contact between the microspheres without affecting the microsphere morphology. The raw material encapsulated and the GRADIENT groups were also sintered using similar process and sintering conditions did not affect the morphology of the scaffolds. The 3D scaffolds had void spaces that were open and interconnected in between the sintered microspheres. The total porosity of the CS and BG scaffolds was attributed to the void space between the sintered microspheres, as well as to the sub micron pores seen on the surface and within the microspheres.

In the present study, the degradation of the scaffolds was not studied specifically; however, we observed morphological changes in the size of the constructs due to swelling and degradation during the culture period as represented in the Table III. The variations in the dimensions of the CS and BG constructs from that of control PLGA group, at different time points indicated that these constructs had different degradation rates.

The mechanical property of PLGA, TGF, and BMP can be correlated to the degradation process. The compressive elastic moduli of these constructs decreased at week 3 time point; at the same time there was a massive increase in the scaffold dimensions from week 0 to week 3 due to excessive swelling. The degradation of the microspheres might have been initiated by week 3, which loosened the contact points where microspheres were sintered to form the 3D scaffolds. This and the excessive swelling at week 3 might have resulted in the decrease of elastic modulus in these constructs. The decrease in dimensions at week 6 could be due to shrinkage or the degradation and the removal of the swollen polymer. At week 6, the scaffolds had a structure that appeared as either closely packed microspheres or a thick polymer mass. The higher packing density of the polymer might have resulted in a higher modulus. The changes in structure of 3D scaffold during the degradation process, might have followed a similar pattern as observed during mechanical compression; as previously reported from our group (Singh et al., 2008).

The compressive elastic moduli of CS and BG constructs did not show a significant change with increase in either GAG collagen or calcium content at week 3. At week 3, the unseeded scaffolds with microspheres containing raw materials will be less stiff when compared to the PLGA scaffold. This is because there is a lower percentage of polymer at each sphere–sphere interface on the sites of sintering than the PLGA that are more strongly sintered together. Hence it was inferred that in the cell-seeded constructs at week 3, the extra cellular matrix secreted by the cells may have counteracted the decreases in moduli generated due to the degradation of the polymer and thereby no changes in modulus were observed.

We observed that the medium containing the control PLGA constructs became more acidic than the medium containing the PLGA-CS and PLGA-BG constructs during the culture period between week 3 and week 6 due to the bulk degradation of PLGA. During the degradation of PLGA, the encapsulated raw materials were slowly released into the culture medium, which helped to regulate the pH of the microenvironment surrounding the cells. The release of BG particles might generate a local alkaline environment that can neutralize the acidic degradation products of PLGA. Similar observations were also reported by Qiu et

al. (2000) in the case of bioglass 45S5 encapsulated PLGA microspheres. During in vivo applications, this might help to reduce the pH drop or even avoid inflammatory reactions caused by pure PLGA. During in vitro culture, medium supplemented with 15 mM HEPES buffer was also added to all of the constructs to maintain the pH. We have previously reported that the cells remain viable even after 3 weeks of culture on the 3D microsphere scaffolds (Singh et al., 2010).

We have not investigated the influence of surface properties of microspheres on initial cell attachment and spreading. Previous reports have shown that the surface roughness of microspheres along with other properties like chemical composition and wettability influence cell adhesion, spreading, proliferation, and differentiation (Kato et al., 2003). To promote pluripotent stem cell attachment (Newman and McBurney, 2004) fabricated PLGA microspheres, with slightly rough and porous surfaces. Deligianni et al. (2001) reported that surface roughness, influenced protein adsorption and ultimately influenced human bone marrow cell behavior. Boyan et al. (2003) reported altered attachment and enhanced differentiation of osteoblast-like cells on rough surfaces in comparison with smoother ones, and suggested that structural features of the surface modulate the expression of phenotypic markers and influence the way cells respond to regulatory factors.

Our results indicated that the release of CS and BG will be highly influenced by the degradation of the polymer and a detailed release pattern of CS was carried out on the unseeded scaffolds. Our data indicated that CS did not rapidly diffuse out of the minute pores present on the surface of the CS microspheres; however when the polymer degraded they were slowly released from the microspheres. The week 0 data indicated that the CS was strongly bound to the polymer and they cannot freely diffuse into the aqueous phase. The week 2 and week 4 data showed an onset of PLGA degradation and represented a degradative phase. At week 6, as the polymer swelled and degraded, the CS was loosely bound to the polymer and more CS was extracted into the aqueous phase. This produced an increase in the CS content in the aqueous phase and decrease in the polymer phase. Thus the data confirmed that degradation of PLGA is necessary to release most of the CS encapsulated in the polymer. The data provided a better understanding of the process of CS release from the microspheres; however they cannot serve as a direct control for the cell-seeded constructs. Dormer et al. (2013) have also reported detailed characterization of protein release over a period of 6 weeks from PLGA and PLGA-HAP microspheres fabricated using similar protocol. This study focused on the effect of different sintering and sterilization methods on the protein release. The microspheres showed a controlled release over a period of 6 weeks.

The week 0 time point (24 hours after cell seeding) is the time for cell attachment and spreading. The biochemical results indicated that the CS group at week 3 had three times more GAGs than at week 0. Furthermore, the GAG content of the CS group at week 3 was around 30 times higher than both the PLGA and TGF groups. These results indicated that the encapsulated raw material had a significant role in enhancing the cellular GAG secretion. The data also indicated that encapsulating CS may be a suitable alternative to expensive growth factors in promoting the secretion of GAGs. The week 6 data could not be directly correlated to the encapsulated raw material, as it was highly dependent on the

degradation of the polymer. In cell-seeded constructs, the degradation and the release profile will also be influenced by the cells and extra cellular matrix already present in the construct at these time points. Measuring GAGs in the acellular constructs over the same period and in culture medium provided more information on this aspect though they cannot be used as a direct control for the cell-seeded constructs. This confirmed that polymer degradation is essential for the release of CS encapsulated within the microspheres. Hence the values obtained from the biochemical analysis attribute mostly to the GAG secreted by the cells and partly to the CS diffused into aqueous phase and entrapped on the ECM. This might be considered as a limitation of the in vitro study. However if the regenerating tissue is able to incorporate and assimilate the CS released from the material, then it will be included as part of the regenerated tissue and they serve as a key strength in vivo, as building blocks of the regenerating tissue.

The results of biochemical analysis indicated that the CS group had 30 times more GAGs than the TGF group. Both the encapsulated and the newly secreted GAGs might have contributed to the enhanced secretion of aggrecan in CS constructs. Previous studies by Huang (1977) have shown that extracellular CS have a modulatory effect on chondrocytes. Wu et al. (2010) have also shown that there was significant increase in proliferation, biosynthesis rate of proteoglycans, and other chondrogenic proteins by exogenous supplement of GAGs when human chondrocytes were grown on 3D scaffolds.

The decrease in both GAG and calcium at the week 6-time point can be explained by correlating the degradation of the microspheres. The PLGA used for the study had an intrinsic viscosity of 0.35 dL/g, and the complete degradation of this polymer in vivo was 12 weeks as per the manufacturer data sheet. We speculate that as the PLGA experienced bulk degradation between weeks 3 and 6, there might have been a higher release of the encapsulated CS into the culture medium that was washed out during the medium change. Even though this was not a favorable situation in vitro, the release of CS may generate a favorable situation in vivo for cartilage regeneration. The GAG, hydroxyproline, and the calcium content estimated was the total amount detected in the whole of the scaffold and was not normalized to the DNA content. The differences in initial cell attachment on the scaffolds and there by the changes in the cell density and cell-cell interactions could have also led to the differences observed in the secretion of matrix components. The total DNA content might have provided better information on the influence of raw material on the cell response.

The immunohistochemistry data at week 6 indicated that the majority of collagen secreted by the TGF-CS was type II, while BG constructs secreted more collagen type I. The very low collagen content in the BMP-BG constructs from the biochemical analysis correlated to the immunohistochemical staining. A combination of both raw material and growth factor TGF-β3 in the microsphere was necessary to accelerate the mesenchymal stem cells' secretion of collagen type II, the major component present in the ECM of hyaline cartilage. More collagen staining was observed in the PLGA and TGF, however very little hydroxyproline was measured on these constructs. On the contrary, there was more hydroxyproline measured in the CS but little collagen I or II detected on the sections. The contradiction could be due to that the hydroxyproline measurement represented the total

collagen present in the whole of a cell-seeded construct and the immunostaining represented the presence of mature collagen on the constructs. Thus the data indicated that the PLGA and the TGF constructs showed deposition of mature collagen, though the total collagen production is less. However, the CS promotes an increase in collagen content but requires more time to mature. Future investigations may be needed to evaluate this in detail.

On the other hand, incorporation of BG in the microspheres resulted in faster mineralization and secretion of collagen that is essential for faster regeneration of bone. The gradient constructs showed cartilage specific molecules in the chondrogenic and higher mineralization in the osteogenic region. The gradient pattern was very evident in the secretion of GAGs and mineralization. However mineralization was also observed in certain regions of the chondrogenic region, this could be due to the formation of hypertrophic cartilage in the vicinity of BG present at the interface region. Asselin et al. have reported that chondrocytes become hypertrophic in presence of BG.

Conclusion

Encapsulating the raw materials CS and BG in PLGA microspheres altered the appearance, structure, porosity, and degradation of the microspheres and provided a buffering effect to cells in culture. Both of the groups encapsulated with chondroitin sulfate (CS and TGF-CS) outperformed the TGF group in total GAG content. They also surpassed the TGF group in collagen production at 6 weeks. Similarly, BG outperformed BMP in collagen and calcium production at 3 weeks, suggesting the raw materials encapsulated in scaffolds alone have the potential of accelerating the cells' secretion of some of the major ECM (though not all) components. The results of the study showed that raw materials can exist as part of the temporary scaffold to create a favorable microenvironment for cells during the repair, and they can be utilized for faster creation of new tissue-specific ECM. Encapsulating raw materials in a gradient pattern for osteochondral regeneration is beneficial. Clear regional variation was confirmed in our results of GRADIENT scaffolds via histology. Thus, 3D scaffolds with simultaneous growth factor and raw material gradients may be highly beneficial in the acceleration of osteochondral regeneration. In addition to the benefits in efficacy with raw materials alone, there is also tremendous clinical significance, as materials that do not include growth factors may be strategically positioned for a shorter and less costly FDA regulatory path as a medical device, and also avoid the high cost of growth factors, which means a larger profit margin, and collectively this leads to greater incentive for investors and entrepreneurs and thus the likelihood of translation to the clinic. This study also revealed the importance of investigating initial cell response on modified microspheres, the release profile of raw materials during the culture and how this is dependent on the degradation of polymer; which we plan to investigate in our future studies.

Supplementary Material

Refer to Web version on PubMed Central for supplementary material.

Acknowledgments

The work was carried out as part of NIH-funded project (R01 AR056347).

References

Berkland C, Kim K, Pack DW. Fabrication of PLG microspheres with precisely controlled and monodisperse size distributions. J Control Release. 2001; 73(1):59–74. [PubMed: 11337060]

Boyan BD, Lossdorfer S, Wang L, Zhao G, Lohmann CH, Cochran DL, Schwartz Z. Osteoblasts generate an osteogenic microenvironment when grown on surfaces with rough microtopographies. Eur Cell Mater. 2003; 6:22–27. [PubMed: 14577052]

Chen YL, Lee HP, Chan HY, Sung LY, Chen HC, Hu YC. Composite chondroitin-6-sulfate/dermatan sulfate/chitosan scaffolds for cartilage tissue engineering. Biomaterials. 2007; 28(14):2294–2305. [PubMed: 17298844]

Deligianni DD, Katsala ND, Koutsoukos PG, Missirlis YF. Effect of surface roughness of hydroxyapatite on human bone marrow cell adhesion, proliferation, differentiation and detachment strength. Biomaterials. 2001; 22(1):87–96. [PubMed: 11085388]

Dormer NH, Busaidy K, Berkland CJ, Detamore MS. Osteochondral interface regeneration of rabbit mandibular condyle with bioactive signal gradients. J Oral Maxillofac Surg. 2011; 69(6):e50–e57. [PubMed: 21470747]

Dormer NH, Singh M, Wang L, Berkland CJ, Detamore MS. Osteochondral interface tissue engineering using macroscopic gradients of bioactive signals. Ann Biomed Eng. 2010; 38(6):2167–2182. [PubMed: 20379780]

Dormer NH, Singh M, Zhao L, Mohan N, Berkland CJ, Detamore MS. Osteochondral interface regeneration of the rabbit knee with macroscopic gradients of bioactive signals. J Biomed Mater Res A. 2012; 100(1):162–170. [PubMed: 22009693]

Dormer NH, Gupta V, Scurto AM, Berkland CJ, Detamore MS. Effect of different sintering methods on bioactivity and release of proteins from PLGA microspheres. Mater Sci Eng Part C. 2013; 33(7): 4343–4351.

Edwards CA, O'Brien WD Jr. Modified assay for determination of hydroxyproline in a tissue hydrolyzate. Clin Chim Acta. 1980; 104(2):161–167. [PubMed: 7389130]

Fan H, Hu Y, Zhang C, Li X, Lv R, Qin L, Zhu R. Cartilage regeneration using mesenchymal stem cells and a PLGA-gelatin/chondroitin/hyaluronate hybrid scaffold. Biomaterials. 2006; 27(26): 4573–4580. [PubMed: 16720040]

Fu Q, Rahaman MN, Bal BS, Bonewald LF, Kuroki K, Brown RF. Silicate, borosilicate, and borate bioactive glass scaffolds with controllable degradation rate for bone tissue engineering applications II. In vitro and in vivo biological evaluation. J Biomed Mater Res A. 2010; 95(1): 172–179. [PubMed: 20540099]

Hench LL, Thompson I. Twenty-first century challenges for biomaterials. J R Soc Interface. 2010; 7(Suppl 4):S379–S391. [PubMed: 20484227]

Hoppe A, Guldal NS, Boccaccini AR. A review of the biological response to ionic dissolution products from bioactive glasses and glassceramics. Biomaterials. 2011; 32(11):2757–2774. [PubMed: 21292319]

Huang D. Extracellular matrix-cell interactions and chondrogenesis. Clin Orthop Relat Res. 1977 Mar-Apr;(123):169–176. [PubMed: 852175]

Kato D, Takeuchi M, Sakurai T, Furukawa S, Mizokami H, Sakata M, Hirayama C, Kunitake M. The design of polymer microcarrier surfaces for enhanced cell growth. Biomaterials. 2003; 24(23): 4253–4264. [PubMed: 12853257]

Lu HH, El-Amin SF, Scott KD, Laurencin CT. Three-dimensional, bioactive, biodegradable, polymer bioactive glass composite scaffolds with improved mechanical properties support collagen synthesis and mineralization of human osteoblast-like cells in vitro. J Biomed Mater Res A. 2003; 64(3):465–474. [PubMed: 12579560]

Mohan N, Dormer NH, Caldwell KL, Key VH, Berkland CJ, Detamore MS. Continuous gradients of material composition and growth factors for effective regeneration of the osteochondral interface. Tissue Eng Part A. 2011; 17(21–22):2845–2855. [PubMed: 21815822]

Newman KD, McBurney MW. Poly(D,L lactic-co-glycolic acid) microspheres as biodegradable microcarriers for pluripotent stem cells. Biomaterials. 2004; 25(26):5763–5771. [PubMed: 15147822]

Qiu QQ, Ducheyne P, Ayyaswamy PS. New bioactive, degradable composite microspheres as tissue engineering substrates. J Biomed Mater Res. 2000; 52(1):66–76. [PubMed: 10906676]

Rahaman MN, Day DE, Bal BS, Fu Q, Jung SB, Bonewald LF, Tomsia AP. Bioactive glass in tissue engineering. Acta Biomater. 2011; 7(6):2355–2373. [PubMed: 21421084]

Renth AN, Detamore MS. Leveraging “raw materials” as building blocks and bioactive signals in regenerative medicine. Tissue Eng Part B Rev. 2012; 18(5):341–362. [PubMed: 22462759]

Singh M, Detamore MS. Stress relaxation behavior of mandibular condylar cartilage under high-strain compression. J Biomech Eng. 2009; 131(6):061008. [PubMed: 19449962]

Singh M, Morris CP, Ellis RJ, Detamore MS, Berkland C. Microsphere-based seamless scaffolds containing macroscopic gradients of encapsulated factors for tissue engineering. Tissue Eng Part C Methods. 2008; 14(4):299–309. [PubMed: 18795865]

Singh M, Sandhu B, Scurto A, Berkland C, Detamore MS. Microsphere-based scaffolds for cartilage tissue engineering: Using subcritical CO2 as a sintering agent. Acta Biomaterialia. 2010; 6(1): 137–143. [PubMed: 19660579]

Will J, Gerhardt LC, Boccaccini AR. Bioactive glass-based scaffolds for bone tissue engineering. Adv Biochem Eng Biotechnol. 2012; 126:195–226. [PubMed: 22085919]

Wu CH, Ko CS, Huang JW, Huang HJ, Chu IM. Effects of exogenous glycosaminoglycans on human chondrocytes cultivated on type II collagen scaffolds. J Mater Sci Mater Med. 2010; 21(2):725–729. [PubMed: 19823917]

Xynos ID, Edgar AJ, Buttery LD, Hench LL, Polak JM. Gene-expression profiling of human osteoblasts following treatment with the ionic products of Bioglass 45S5 dissolution. J Biomed Mater Res. 2001; 55(2):151–157. [PubMed: 11255166]

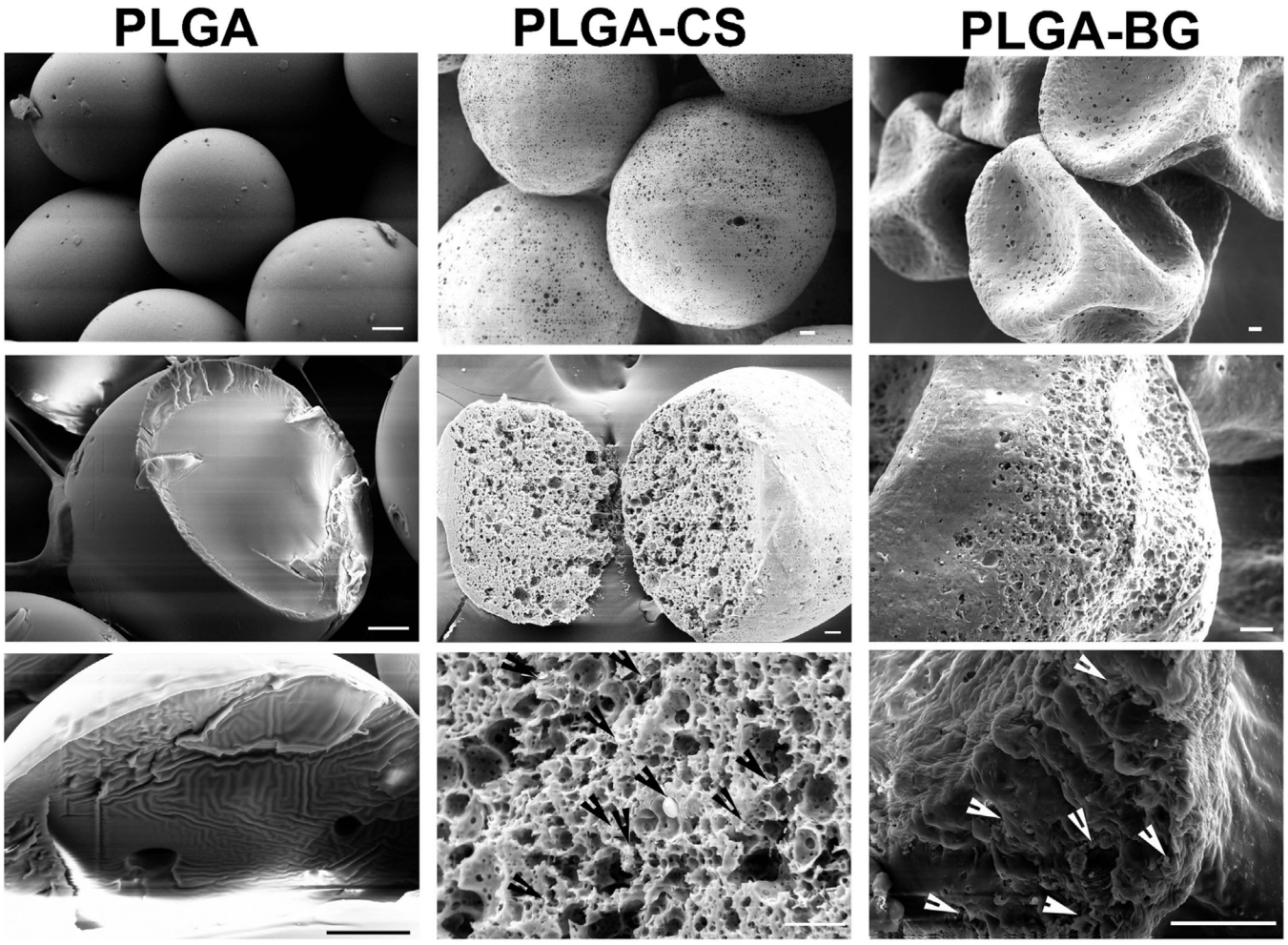

Figure 1.

Scanning electron micrographs (SEM) of microspheres prior to the fabrication of scaffolds. The images in the top panel from each column demonstrate the morphology of the surface; the middle and the lower panels demonstrate the cross section of cryofractured microspheres. PLGA microspheres had smooth surfaces, whereas the microspheres with encapsulated CS or bioactive glass had porous surfaces. The PLGA-BG microspheres had the structure of a deflated soccer ball after lyophilization. The arrows in the lower panel in PLGA-CS and PLGA-BG point to the chondroitin sulfate and bioactive glass particles deposited inside the microspheres. Scale bars: 20 μm. PLGA poly(D,L-lactic-co-glycolic acid), PLGA-CS poly(D,L-lactic-co-glycolic acid-chondroitin sulfate), PLGA-BG (poly(D,L-lactic-co-glycolic acid)-bioactive glass).

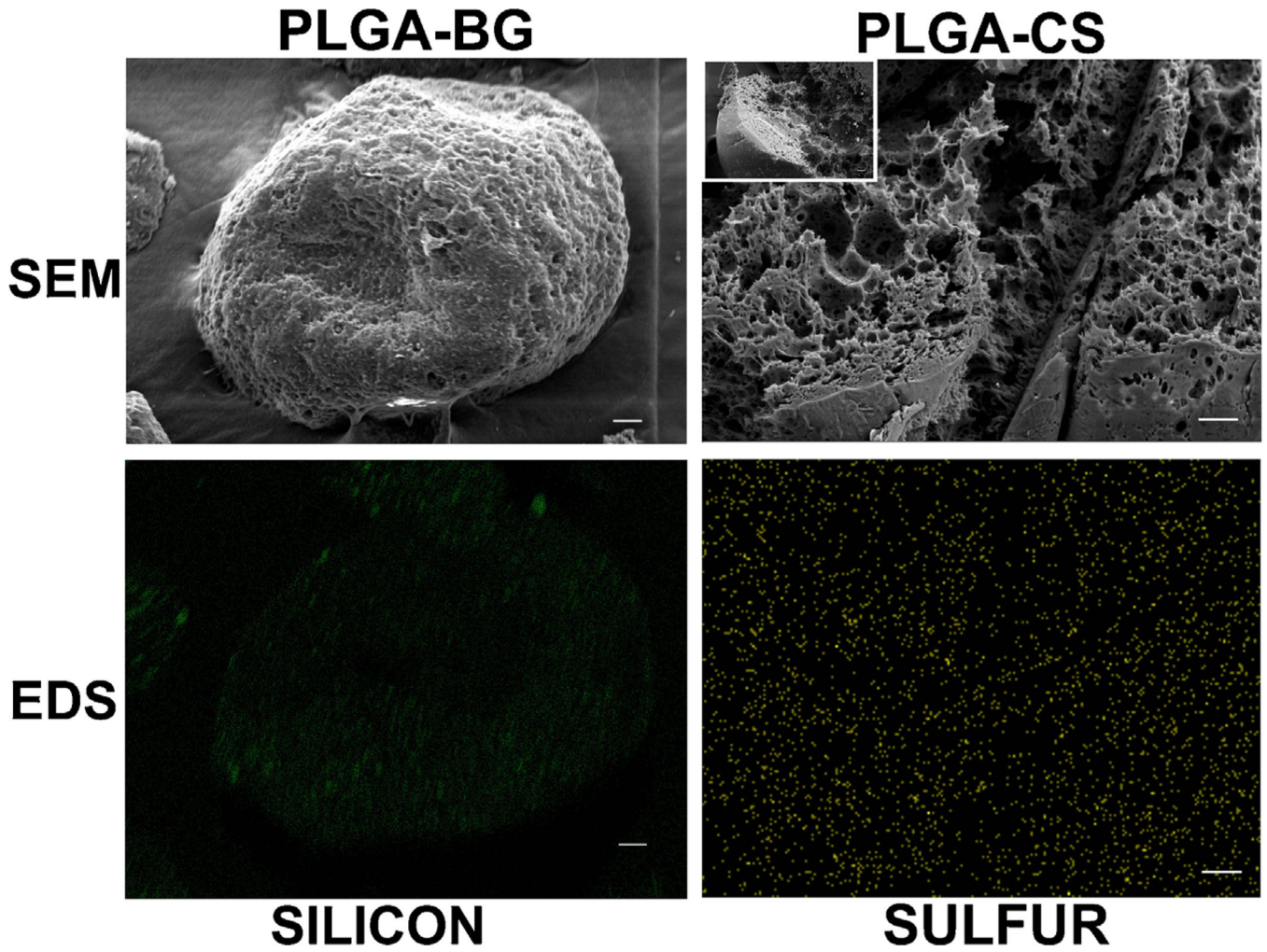

Figure 2.

Scanning electron micrographs (SEM) and energy dispersive system (EDS) mapping of microspheres prior to sintering showing the distribution of BG in PLGA-BG and CS in PLGA-CS. The left panels indicate SEM of the surface of a PLGA-BG microsphere and EDS mapping for silicon (green color) to identify the distribution of BG nanoparticles on the surface of the microsphere. Similarly, the right panels correspond to SEM and EDS mapping for sulfur (yellow color) in the cross section of a cryofractured PLGA-CS microsphere. Distribution of BG and CS were nearly—but not perfectly—homogeneous. Scale bars: 20 μm. PLGA-CS poly(D,L-lactic-co-glycolic acid-chondroitin sulfate), PLGA-BG poly(D,L-lactic-co-glycolic acid-bioactive glass), CS (chondroitin sulfate) and BG (bioactive glass).

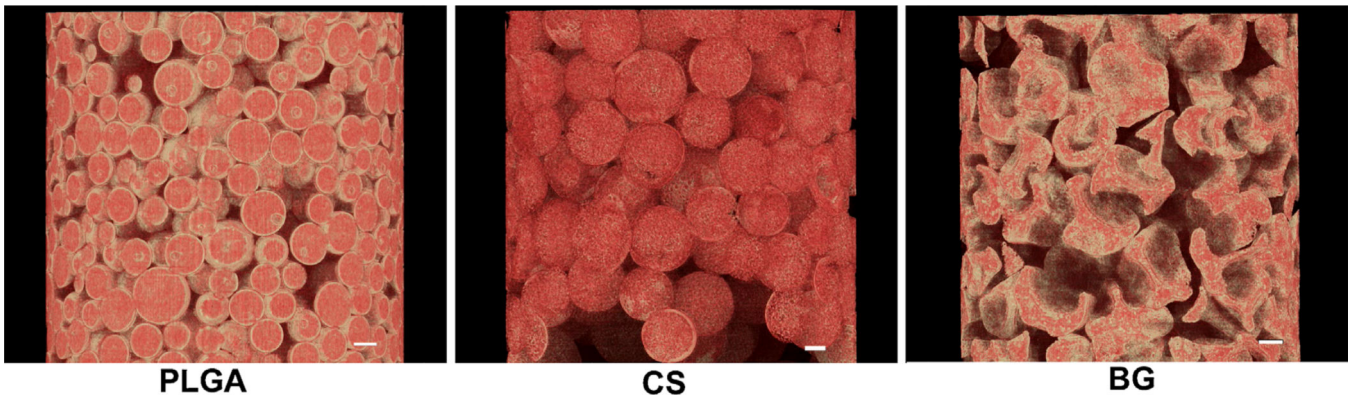

Figure 3.

The 3D reconstructed microCT images represent a region within the 3D microsphere-based scaffolds. The images indicate that the scaffolds have a structure with open interconnected pores and also show the porous structure inside of the PLGA-CS and PLGA-BG microspheres. These microCT images are highly consistent with the morphology observed via SEM (Fig. 1). Scale bars: 100 μm. PLGA-CS poly(D,L-lactic-co-glycolic acid-chondroitin sulfate), PLGA-BG poly(D,L-lactic-co-glycolic acid-bioactive glass).

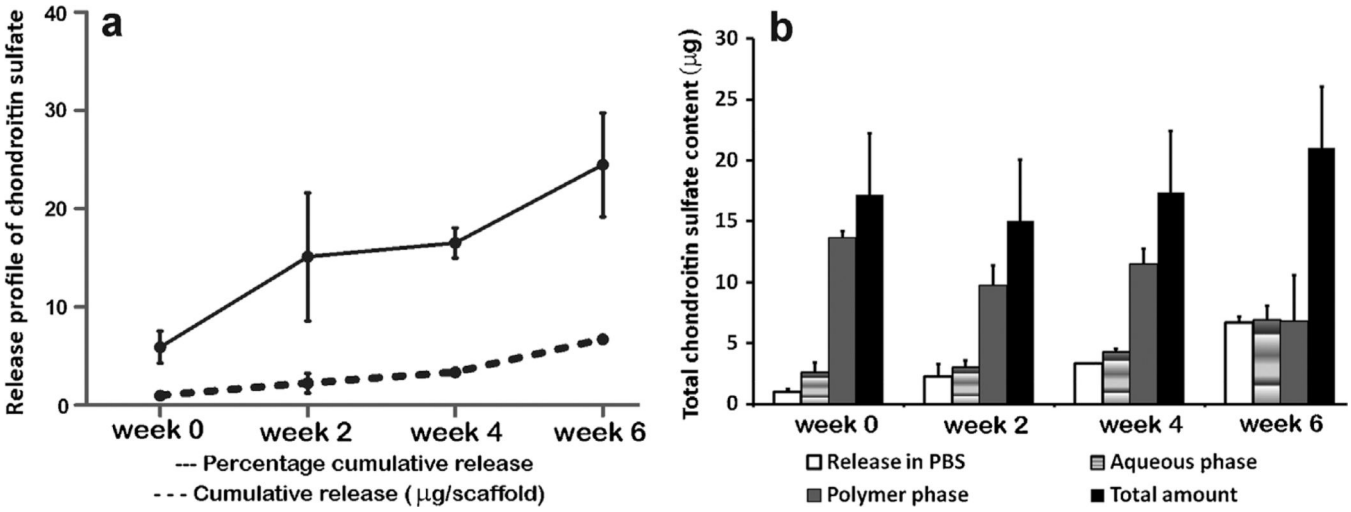

Figure 4.

a: The release profile of chondroitin sulfate from the unseeded CS scaffolds. **b:** The amount of CS released and retained within the scaffolds at week 0, week 2, week 4, and week 6. Values are reported as mean ± of standard deviation, $n = 3–4$.

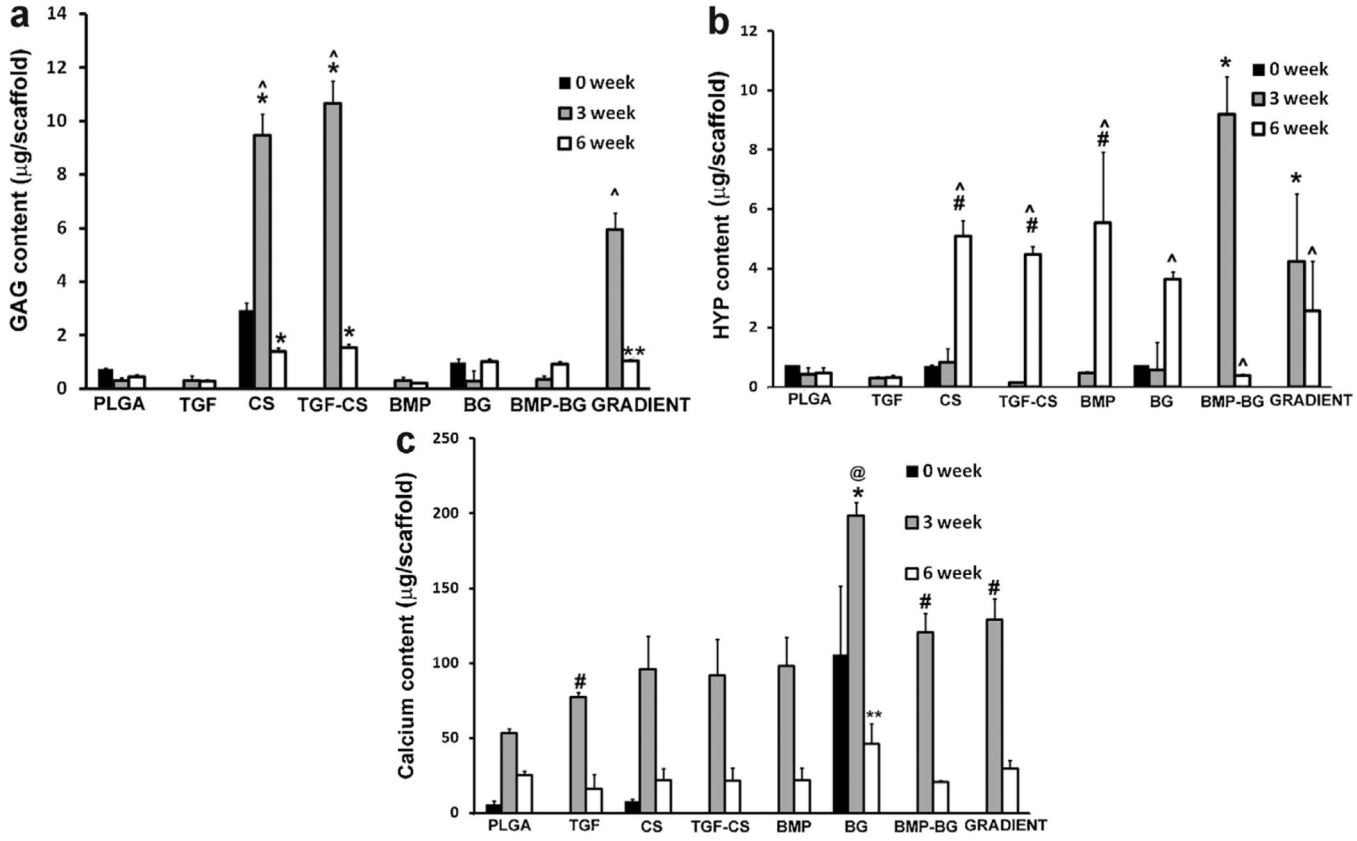

Figure 5.

a: Glycosaminoglycan contents of rBMSC-seeded scaffolds at different time points. The values at week 0 indicate 24 h after cell seeding (measured only for three scaffold types: PLGA, CS, and BG). Values are reported as mean ± standard deviation (n = 3–4), $P < 0.05$. *Statistically significant difference from all other groups; however, there was no significant difference between CS and TGF-CS at any given time point, **statistically significant difference from groups PLGA and the growth factor loaded constructs at week 6 and ^statistically significant difference from week 6 within a group. **b:** HYP (hydroxyproline) contents in rBMSC-seeded scaffolds at different time points. The BMP-BG constructs showed significantly higher values than the other groups at week 3; however, a significant decrease was observed at week 6 in contrast, multiple groups saw a drastic increase from week 3 to week 6. *Statistically significant difference from all other groups at week 3, #statistically significant difference from PLGA, TGF, and BMP-BG at week 6 and ^statistically significant difference from previous week. **c:** Calcium contents in rBMSC-seeded scaffolds at different time points. The PLGA-BG constructs showed significantly higher values than all other groups at week 3. *Statistically significant difference from all other groups at week 3, #statistically significant difference from PLGA at week 3, **statistically significant difference from all groups except PLGA and GRADIENT at week 6, @statistically significant from 6-week time point. PLGA poly($_{D,L}$-lactic-co-glycolic acid), CS (chondroitin sulfate), BG (bioactive glass), TGF-CS (transforming growth factor-chondroitin sulfate), and BMP-BG (bone morphogenic protein-bioactive glass).

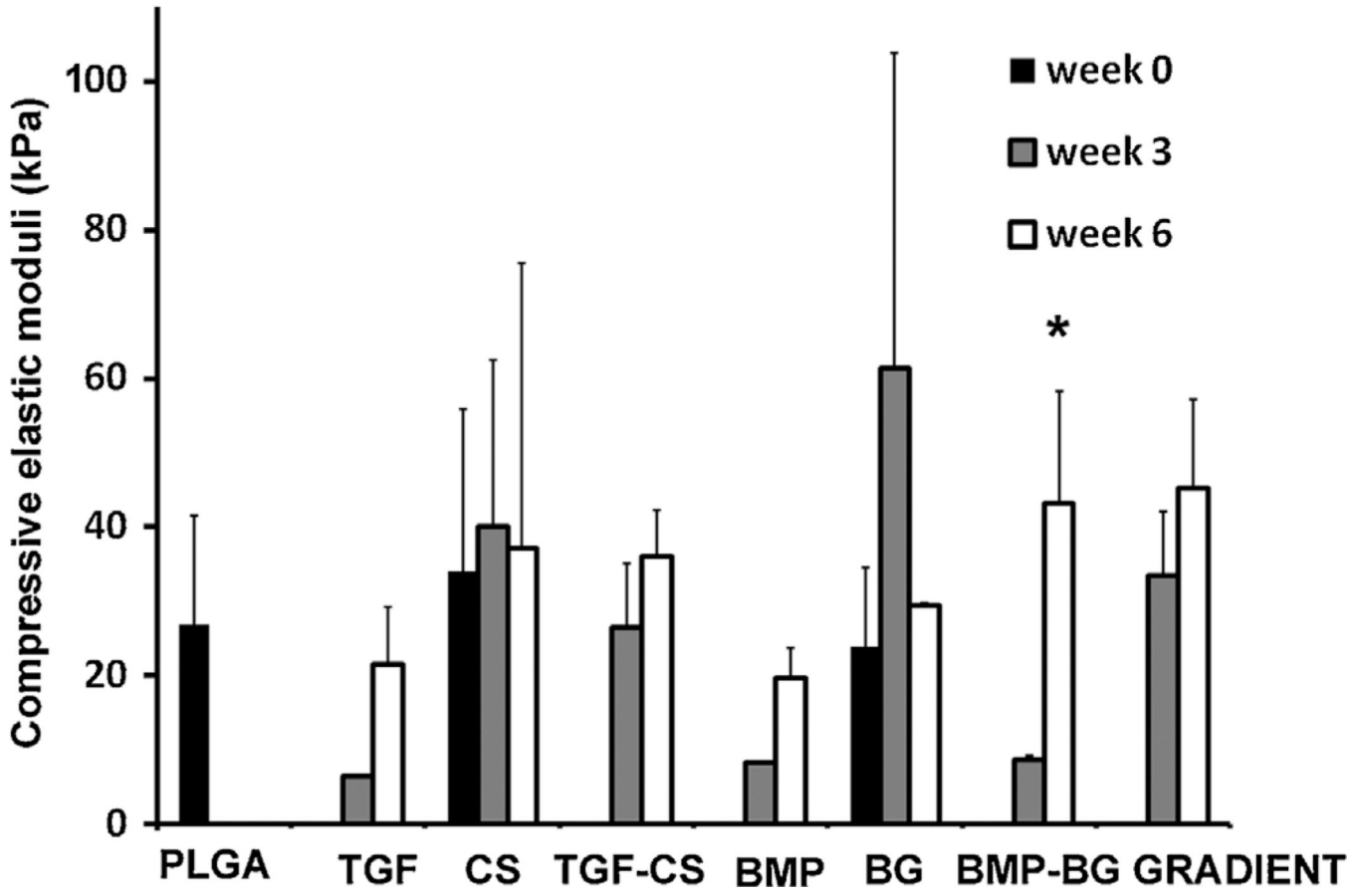

Figure 6.

The compressive elastic moduli of unseeded PLGA, CS, and BG scaffolds at week 0 and constructs at week 3 and week 6. Values are reported as mean ± of standard deviation, $n = 3$. Control PLGA scaffolds did not possess sufficient structural integrity to allow for compression to be performed at week 3 and week 6. *Statistically significant from the previous time point, $p < 0.05$. There was no significant difference among groups at a given time point according to the ANOVA, so no post hoc analyses were performed. PLGA poly(D,L-lactic-co-glycolic acid), CS (chondroitin sulfate), BG (bioactive glass).

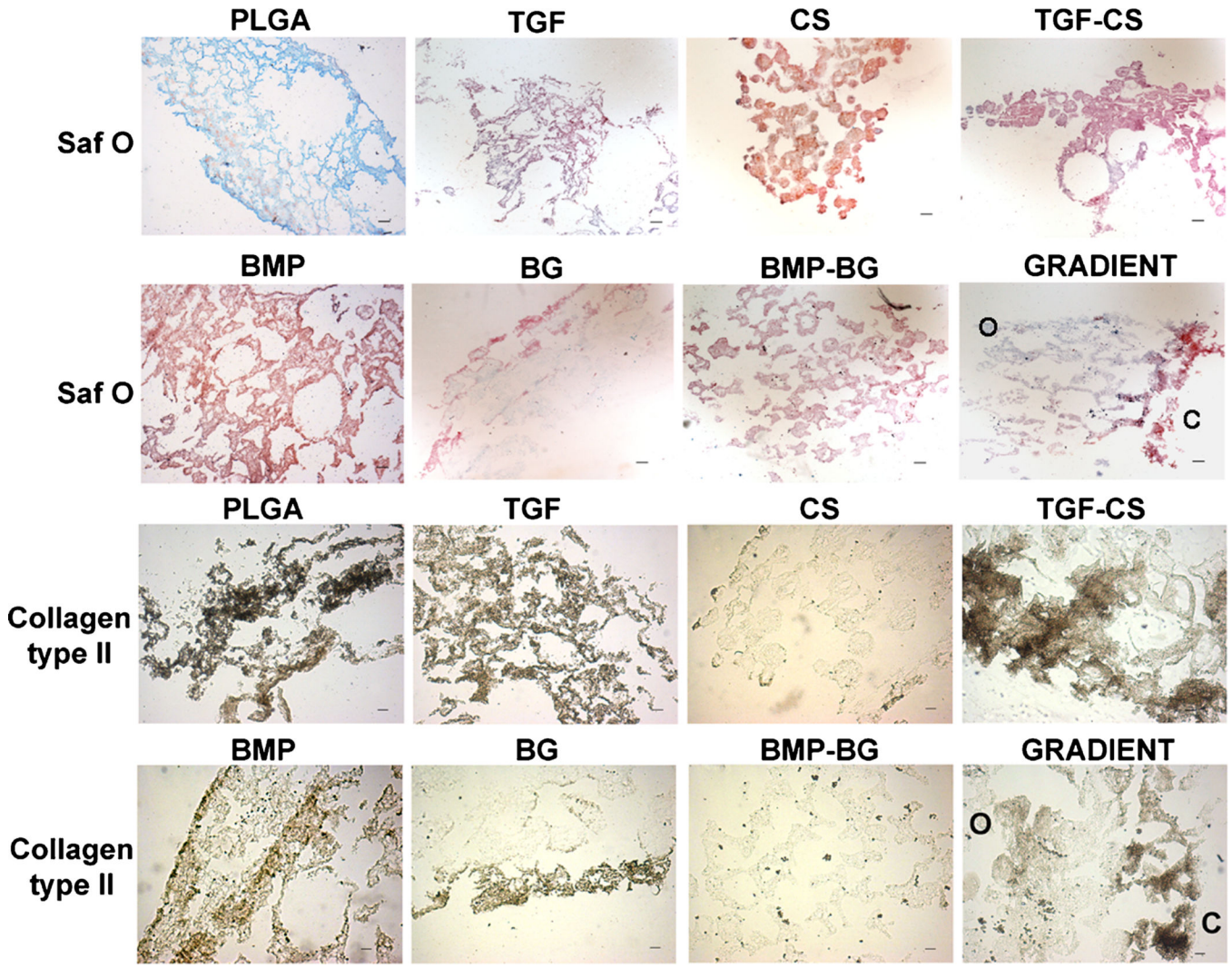

Figure 7.

Representative images for histological analysis of constructs at week 6. The CS encapsulated groups showed deeper staining for Safranin O. The immunostaining intensity for collagen type II was greater in the TGF group. The gradient scaffolds showed more intense staining for GAG and collagen type II in the chondrogenic region. C and O represent the locations of the chondrogenic and osteogenic sides on the sections of gradient scaffolds. Scale bar: 100 μm. PLGA poly(D,L-lactic-co-glycolic acid), TGF (transforming growth factor-β3), CS (chondroitin sulfate), TGF-CS (transforming growth factor-chondroitin sulfate), BMP (bone morphogenic protein-2), BG (bioactive glass), and BMP-BG (bone morphogenic protein-bioactive glass).

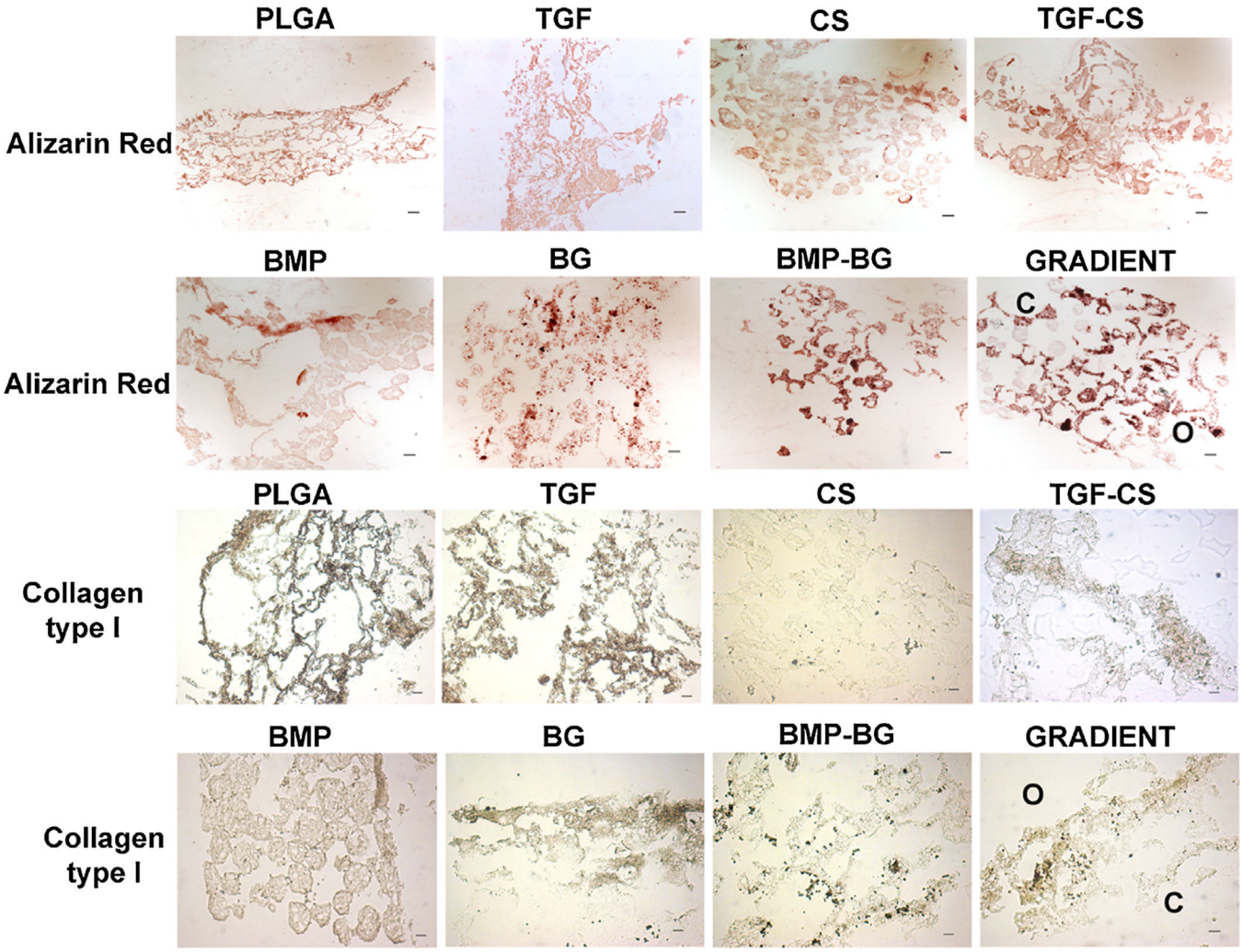

Figure 8.

Representative images for histological analysis of constructs at week 6. The BG encapsulated groups showed deeper staining for Alizarin red. The immunostaining intensity for collagen type I was greater in the TGF group. The gradient scaffolds showed more intense staining that indicated higher mineralization toward the osteogenic region. However, mineralization was observed at a few locations in the chondrogenic region of the gradient construct. C and O represent the locations of the chondrogenic and osteogenic sides on the sections of gradient scaffolds. Scale bar: 100 μm. PLGA poly(D,L-lactic-co-glycolic acid), TGF (transforming growth factor-β3), CS (chondroitin sulfate), TGF-CS (transforming growth factor-chondroitin sulfate), BMP (bone morphogenic protein-2), BG (bioactive glass), and BMP-BG (bone morphogenic protein-bioactive glass).

Table I

The scaffolds, type of microspheres and the composition of each microsphere.

Scaffolds	Type of microsphere used in each scaffold	Contents
Control		
PLGA	PLGA	PLGA
Chondrogenic		
TGF	PLGA-TGF	PLGA, TGF-β3
CS	PLGA-CS	PLGA, chondroitin sulfate
TGF-CS	PLGA-TGF-CS	PLGA, TGF-β3, chondroitin sulfate
Osteogenic		
BMP	PLGA-BMP	PLGA, BMP-2
BG	PLGA-BG	PLGA, bioactive glass
BMP-BG	PLGA-BMP-BG	PLGA, BMP-2, bioactive glass
GRADIENT	PLGA-TGF-CS	PLGA, TGF-β3, chondroitin sulfate
	PLGA-BMP-BG	PLGA, BMP-2, bioactive glass

Table II

Experimental design.

Groups	PLGA			CS			TGF-CS			BMP			BG			BMP-BG			GRADIENT	
SEM of microspheres	x			x			—			—			x			—			—	
EDS of microspheres	—			x			—			—			x			—			—	
MicroCT of 3D scaffolds	x			x			—			—			x			—			—	
Cell culture weeks	**0**	**3**	**6**	**0**	**3**	**6**	**0**	**3**	**6**	**0**	**3**	**6**	**0**	**3**	**6**	**0**	**3**	**6**	**0**	**3**	**6**
Biochemical	x	x	x	x	x	x	—	x	x	—	x	x	x	x	x	—	x	x	—	x	x
Mechanical testing	x	—	—	x	x	x	—	x	x	—	x	x	x	x	x	—	x	x	—	x	x
Histology	—	—	x	—	—	x	—		x	—	—	x	—	—	x	—	—	x	—	—	x

The analyses used for characterization of microspheres, 3D scaffolds, and cell-seeded constructs (x denotes performed, - denotes the analysis is not perfomed).

Table III

The dimensions of the constructs used for mechanical testing.

	Dimensions (mm), diameter (D), and height (h)			Volume (mm^3)		
Scaffold	**0 week**	**3 week**	**6 week**	**0 week**	**3 week**	**6 week**
PLGA						
(D)	4.45±0.03			123±18		
(h)	7.9±1.2					
TGF						
(D)		10[a]	7.25±0.31[a]		656±42	125±37
(h)	—	7.98±0.76	3.03±0.86[a]			
CS						
(D)	3.22±0.16	6.5±0.14[b]	4.63±0.55[b]	41±11	272±22	107±21
(h)	4.7±1.2	8.2±1.0[b]	6.35±0.40			
TGF-CS						
(D)		6.6±0.08[b]	4.4±0.6[b]		278±13	86±15
(h)	—	7.88±0.34[b]	5.71±0.44			
BMP						
(D)		8[a]	6[a]		428±9	117±42
(h)	—	8.4±0.3	4.2±1.5[a]			
BG						
(D)	4.7±0.1	9[a]	8.1		805±2	484±72
(h)	6.70±0.38	13.3±1.1[b]	9.4±1.4	116±6		
BMP-BG						
(D)		6.6±0.6[a]	5		303±37	93±23
(h)	—	8.1	4.7±1.2			
GRADIENT						
(D)		7[b]	5.17±0.46		340±32	124±34
(h)	—	8.7±1.0	5.83±0.72			

Scaffolds without growth factors were used for week 0 analysis. Values represented are averages + standard deviation of $n = 3$, $P < 0.05$.

[a] Statistically significant difference from week 0 PLGA samples.

[b] Statistically significant difference from the respective raw material supplemented group at week 0.